DEUTSCHES ELEKTRONEN – SYNCHROTRON

DESY 92-022
February 1992

Matrix Element Calculation of Quark Bremsstrahlung in $O(\alpha\alpha_s)$

G. Kramer, H. Spiesberger

II. Institut für Theoretische Physik, Universität Hamburg

ISSN 0418-9833

NOTKESTRASSE 85 · D-2000 HAMBURG 52

To be sure that your preprints are promptly included in the
HIGH ENERGY PHYSICS INDEX,
send them to the following (if possible by air mail):

DESY Bibliothek Notkestraße 85 W-2000 Hamburg 52 Germany	DESY-IfH Bibliothek Platanenallee 6 O-1615 Zeuthen Germany

DESY 92-022
February 1992

ISSN 0418-9833

Matrix Element Calculation of Quark Bremsstrahlung in $O(\alpha\alpha_S)$[1]

G. Kramer and H. Spiesberger[2]
II. Institut für Theoretische Physik der Universität Hamburg,
Luruper Chaussee 149, DW-2000 Hamburg 50, Germany
February 19, 1992

1 Abstract

We describe a matrix element calculation up to $O(\alpha_S)$ of the partial widths of the decay $Z \to \gamma + n\ jets$. Numerical results are given as a function of the invariant mass cut parameter y. A Monte Carlo implementation of the matrix element calculation is described which allows to study the dependence on schemes defining jet resolution and photon isolation.

2 Introduction

This report consists of two parts: the talk of G. Kramer on results of a matrix element calculation of quark bremsstrahlung up to $O(\alpha\alpha_s)$ based on work done in collaboration with B. Lampe and the talk of H. Spiesberger on Monte Carlo studies based on this matrix element calculation.

The main motivation for the calculation of higher order QCD corrections to $e^+e^- \to q\bar{q}\gamma$ is to obtain information on the weak coupling constants of up and down type quarks by comparing to experimental data [1]. Further details on this are given in the contributions of C. Markus and P. Mättig [2,3].

The aim of the theoretical work is the calculation of the partial widths $\Gamma(Z \to \gamma + n\,jets)$ with $n = 1, 2, 3$ up to $O(\alpha\alpha_s)$. These widths are written in the following form

$$\frac{\Gamma(Z \to \gamma + njets)}{\Gamma(Z \to hadrons)} = N g_n(y) \tag{1}$$

where

$$N = \frac{\frac{8}{9}c_u + \frac{1}{3}c_d}{2c_u + c_d}\frac{\alpha}{2\pi}\left(1 + \frac{\alpha_s}{\pi} + 1.42\left(\frac{\alpha_s}{\pi}\right)^2\right)^{-1} \tag{2}$$

[1] Talks presented at the workshop on "Photon radiation from quarks", Annecy, Dec. 2 - 3, 1991
[2] Supported by Bundesministerium für Forschung und Technologie, 05 5HH91P/8, Bonn, Germany

with

$$c_f = v_f^2 + a_f^2 \tag{3}$$

and v_f and a_f are the weak vector and axial vector couplings which are

$$v_f = 2\,I_{3,f} - 4\,Q_f\,s_W^2\,, \quad a_f = 2\,I_{3,f}\,. \tag{4}$$

$I_{3,f}$ is the weak isospin, Q_f the quark charge and $s_W = \sin\theta_W$ with θ_W being the weak mixing angle. α_s is the strong coupling constant.

The partial decay rates $\Gamma(Z \to \gamma + n\,jets)$ depend on jet and photon resolution parameters for which we take the invariant mass cut. This is defined with respect to the invariant mass squared $y_{ij} = (p_i + p_j)^2/s$ ($\sqrt{s} = E_{cm} = M_Z$). $i, j = 1, 2, 3, 4$ where $i = 1(2)$ labels the quark (antiquark), $i = 3$ the photon, and $i = 4$ the additional gluon. In the first part of this report we use the same resolution parameter y for the separation of the photon from the partons (or jets) as for defining jets out of two or three partons. This restriction on the choice of the resolution parameter on the photon and for the jets has the advantage that methods and results of an earlier calculation of n-jet-production rates in e^+e^- annihilation by one of the authors and B. Lampe [4] could be easily applied. These n-jet-rates (n=2,3,4) have been used for the interpretation of PETRA, PEP, TRISTAN, SLC and LEP data with the goal to determine the strong coupling constant α_s.

The results for $g_n(y)$, $n = 1, 2, 3$, have been obtained by G. Kramer and B. Lampe and are published in ref. [5]. To $O(\alpha\alpha_s)$ $g_3(y)$ has only tree graph contributions. $g_2(y)$ and $g_1(y)$ have contributions from lowest order ($O(\alpha)$) and from higher order QCD corrections $O(\alpha\alpha_s)$.

3 Decay Rates into One Photon plus Jets

First we consider the decay rate $Z \to \gamma + 3\ jets$. The photon is isolated from the three jets which are just the three partons: quark(q), antiquark($\bar{q}$) and gluon(g) and we require $y_{ij} \geq y$ for all $i, j = 1, 2, 3, 4$. The reduced rate $g_3(y)$ as defined in (1) is $O(\alpha_s)$ and is written

$$g_3(y) = \frac{\alpha_s}{2\pi}\,g_3^{(1)}(y). \tag{5}$$

$g_3^{(1)}(y)$ is simple to calculate. Results can be found already in in the earlier work [4] where 4-jet rates were computed as a function of a y cut. $g_3^{(1)}(y)$ is just the C_F^2-part of σ_{4-jet}, i.e. the rate for $e^+e^- \to q\bar{q}gg$ with $\alpha_s^2 C_F^2$ replaced by $\alpha\alpha_s C_F$ and the statistical factor $1/2$ removed which occurs in σ_{4-jet} because of two identical gluons. Results for $g_3^{(1)}(y)$ are found in table 2 of ref. [5] for y values between 0.005 and 0.14. $g_3^{(1)}$ is very small for the larger y values. But for small y the rate is appreciable. Note that there are no $q\bar{q}\gamma g$ final states possible for $y \leq 0.16$.

Next we consider the rate for the decay of the Z into a photon plus two jets. The photon is again isolated from the two jets by requiring a minimum invariant mass squared ys between the photon and either of the two jets. In lowest order of QCD the hadronic final state is $q\bar{q}$ (see Fig. 1). We denote the momenta in the decay $Z \to q\bar{q}\gamma$ by p_1, p_2, p_3 respectively and define as usual

$$y_{ij} = (p_i + p_j)^2/s, \tag{6}$$

$i, j = 1, 2, 3$, and the normalized energies of q, $\bar{q}$ and γ in the c.m. system by x_1, x_2 and x_3:

$$x_i = \frac{2E_i}{E_{cm}}, \quad x_1 = 1 - y_{23}, \quad x_2 = 1 - y_{13}, \quad x_3 = 1 - y_{12}. \tag{7}$$

The lowest order differential cross section is well-known

$$\frac{d^2\sigma}{dx_1 x_2} \sim \frac{x_1^2 + x_2^2}{(1-x_1)(1-x_2)}. \tag{8}$$

We write the reduced $\gamma + 2$ *jet*-rate as

$$g_2(y) = g_2^{(0)}(y) + \frac{\alpha_s}{2\pi} g_2^{(1)}(y) \tag{9}$$

and a similar decompostion will be used later for $g_1(y)$. Then $g_2^{(0)}(y)$ is easily calculated numerically from (8) by imposing the constraints $y_{12}, y_{13}, y_{23} \geq y$. The result for various y values between 0.005 and 0.20 is tabulated in table 1 of [5]. Of course from kinematical reasons $y \leq 1/3$ for three massless particles in the final state.

Now we consider the $O(\alpha_s)$ corrections to $g_2(y)$ denoted by $g_2^{(1)}(y)$ in (9). The calculation is very similar to the calculation of the $O(\alpha_s^2)$ correction to σ_{3-jet} [4]. The $O(\alpha\alpha_s)$ correction (if we include the electromagnetic coupling of the quarks) consists of three parts: (i), (ii) and (iii).

(i) The first part contains the singular part of the real contributions of the infrared/collinar singular region defined below and the virtual corrections.

(ii) Part (ii) denotes the remaining non-singular contributions in this same region.

(iii) The third part results from the integration over the phase space region with isolated photons and partons.

First let us consider the real contributions. An example of a photon-3-parton diagram is shown in Fig. 2. The differential rate for $Z \to q\bar{q}\gamma g$ has in general the form

$$d^5\Gamma \sim \Gamma_4^{(0)} = \frac{\alpha_s}{2\pi} f(y_{ij}) dPS(4) \tag{10}$$

This rate must be integrated over different phase space regions to obtain the contributions $g_1^{(1)}(y)$, i.e. the $O(\alpha_s)$ corrections to $\gamma + 1\,jet$, $g_2^{(1)}(y)$, i.e. the $O(\alpha_s)$ corrections to $\gamma + 2\,jets$. $g_3^{(1)}(y)$, the lowest order contribution to $\gamma + 3\,jets$, was already considered above. $\Gamma_4^{(0)}$ contains pole terms proportional to $y_{13}^{-1}, y_{14}^{-1}, y_{23}^{-1}$ and y_{24}^{-1} which are separated by partial fractioning (see [4] for details):

$$f(y_{ij}) = \frac{A_{14}}{y_{14}} + (1 \leftrightarrow 2) + (4 \leftrightarrow 3) + (1 \leftrightarrow 2, 4 \leftrightarrow 3) \tag{11}$$

The terms proportional to y_{14}^{-1} and y_{24}^{-1} contain the QCD singularity, where the gluon is infrared and/or collinear with the quark or antiquark respectively. They give the main terms to the $O(\alpha_s)$ correction of $e^+e^- \to \gamma + 2\,jets$ and must be integrated over the unresolved regions $y_{14} \leq y$ and $y_{24} \leq y$ respectively where qg or $\bar{q}g$ are recombined into one jet. The terms in (11) are separarted into so-called singular terms and non-singular terms. The singular terms are regularized by dimensional regularization. The singularities after integration compensate against the singularities in the $O(\alpha_s)$ one-loop corections to $e^+e^- \to q\bar{q}\gamma$. The integration is done analytically to isolate the remaining finite terms. This result is the contribution (i) referred to above. The terms with the pole terms y_{13}^{-1} and y_{23}^{-1} contain the QED singularities. If integrated over the unresolved regions $y_{13}, y_{23} \leq y$ they contribute to the radiative corrections of $e^+e^- \to 3\,jets$. The resulting singularities in dimensional regularization cancel against the $O(\alpha)$ virtual

corrections to $e^+e^- \to q\bar{q}g$ and do therfore not contribute to the calculation we are interested in here. Since γ and g are distinct the total virtual $O(\alpha\alpha_s)$ corrections are doubled as are the total $e^+e^- \to q\bar{q}\gamma g$ terms as compared to $e^+e^- \to q\bar{q}gg$ in [4]. Compared to the results in [4] the factor $\alpha_s^2 C_F^2$ is replaced by $\alpha\alpha_s C_F$. There is no extra factor 2 since one half of the real contributions and of the total virtual terms of $O(\alpha\alpha_s)$ go into the radiative corrections to $\sigma_{3-jet}(y)$.

The other two contributions (ii) and (iii) come exclusively from the real diagrams in Fig. 2. The second part (ii) consists just of the non-singular terms in A_{14}/y_{14} and A_{24}/y_{24} in (11) which are integrated over the unresolved regions $y_{14} \leq y$ and $y_{24} \leq y$, respectively. They are calculated by numerical integration methods and do not take part in the real-virtual cancellation. The third part (iii) is concerned with the resolved photon regions $y_{13} \geq y$ and $y_{23} \geq y$. In these regions also the qg or $\bar{q}g$ recombination must be done to obtain just two jets. This is done by Monte Carlo integration since the phase space of the unresolved qg and $\bar{q}g$ regions is rather complicated. A further complication arises when we separate the $\gamma + 2\,jets$ from the $\gamma + 1\,jet$ contribution since the definition of the $q\bar{q}\gamma$ variables out of the $q\bar{q}\gamma g$ variables is not unique. As in [4] we consider the two schemes: (1) the KL-scheme where y_{134} and y_{23} ($y_{ijk} = (p_i + p_j + p_k)^2/s$) are defined as new jet-jet-photon-variables. Then according to the 3-parton-photon kinematics the third variable is $y_{124} - y_{14}$ (and equivalently for $1 \leftrightarrow 2$ exchange). The other scheme is the KL' scheme where the jet-jet-photon variables are y_{134} and y_{124} together with $y_{23} - y_{14}$ according to the 3-parton-photon constraint.

We note that compared to the analogous calculation of σ_{3-jet} the two bosons, photon and gluon, are not recombined in the region (iii): $y_{13} \geq y$ since this is now part of the radiative QED corrections. Besides the photon resolved part ($y_{13} \geq y$) we have non-singular contributions from $y_{14} \geq y$ in the term A_{14}/y_{14} in (11) where the antiquark $\bar{q}$ is recombined with the gluon ($y_{24} \leq y$) and where the quark q and the antiquark $\bar{q}$ are in the unresolved region: $y_{12} \leq y$. These two contributions are also counted as part of the region (iii). Except for the $y_{34} \leq y$ region the sum of the non-singular contributuions in (iii), i.e. the terms coming from the two areas $y_{13} \geq y$ and $y_{14} \geq y$, is equal to the analogous non-singular contribution in σ_{3-jet}. Actually this is not quite true. The contribution where quark and antiquark are combined in one jet occurs twice, namely in the $y_{14} \geq y$ part, just mentioned, and in the $y_{13} \geq y$ part considered first. Since the quark-antiquark recombination term is very small we counted it only once.

The sum of parts (i), (ii) and (iii) gives $g_2^{(1)}(y)$. Numerical results are found in table 2 of [5] for the KL' scheme and in table 3 of [5] for the KL scheme for y values between 0.005 and 0.20. From these results we see that $g_2^{(1)}(y)$ is negative for all y values in KL' and changes sign to positive values for KL near $y = 0.055$. For very small y values the $O(\alpha_s)$ correction to $g_2(y)$ is so large that higher order corrections in α_s are expected to become important, too. For $y \geq 0.05$ the $O(\alpha_s)$ correction is moderate or small.

To get an idea about the scheme dependence of $g_2^{(1)}(y)$, we have plotted $g_2^{(1)}(y)$ as a function of y for the two schemes KL and KL' in Fig. 3 and compare it with the $O(\alpha_s^2)$ coefficient of $\sigma_{3-jet}(y)$, denoted by $g_{32}(y)$ for those y values where results are given in [4]. We see that these coefficients $g_2^{(1)}(y)$ and $g_{32}(y)$ differ in the two schemes by approximately the same amount. In $g_{32}(y)$ the difference is somewhat larger because there are additional contributions from the colour factor $C_F N_c$. We remark that the scheme dependence KL and KL' is equivalent to the recombination dependence well-known from 2- and 3-jet rate calculations [7,9,8].

$g_2^{(1)}(y)$ is fairly small for $y \geq 0.05$. For example in the KL' scheme the $(\gamma + 2\,jet)$-rate is changed only by 15% at $y = 0.05$ with $\alpha_s = 0.12$. Therefore the $(\gamma + 2\,jet)$-rate for $y \geq 0.05$

seems well suited for the determination of the weak coupling constants of up and down type quarks [6].

The evaluation of the $O(\alpha\alpha_s)$ correction to $g_1(y)$ is more involved. The contributions originating from the part (i) defined above and also from the part (ii) which are the non-singular contributions in the same region are easy to calculate. In terms of the $q\bar{q}\gamma$ invariant mass variables y_{12}, y_{13}, y_{23} this involves integration over the region $y_{13}, y_{23} \geq y$ and $y_{12} \leq y$ which is the same region from which the lowest order $(\gamma + 1\,jet)$-rate is calculated. This lowest order contribution is $g_1^{(0)}(y)$, where the jet consists just of the combination of q and $\bar{q}$ with the given y resolution parameter. In this approximation there is only the $q\bar{q}$ system recoiling against the high energy photon. This contribution is tabulated in table 1 of [5]. It is very small except for large y cuts where $g_1^{(0)}(y)$ and $g_2^{(0)}(y)$ become comparable. $g_1^{(0)}(y)$ must vanish for $y \to 0$, since there are no singularities in the 1-jet-region in lowest order. Concerning the $O(\alpha_s)$ corrections in the part (i) and (ii) we note that first the gluon is recombined with either the quark or antiquark and then in a second step the region where qg and $\bar{q}$ or q and $\bar{q}g$ are unresolved is integrated out to obtain the $\gamma + 1\,jet$ contribution. It is clear that the result depends on the scheme KL and KL', respectively. The singular part (i) gives the dominant contribution. In the second non-singular part (iii) it is difficult to select $\gamma + 1\,jet$ phase space region, so that double counting is avoided. For a complete calculation, the higher order corrections together with the two-loop virtual corrections must be included. Therefore we considered only the contributions from region (i) and (ii), since the contribution from (i) will also be dominant compared to (iii). Results for the KL' scheme are in table 2 and for the KL scheme in table 3 of [5]. For $y \geq 0.05$ the $O(\alpha_s)$ corrections are positive in both cases. For KL the corrections are larger than for KL'.

Of course all three decay rates $g_1(y), g_2(y)$ and $g_3(y)$ depend on the value of α_s. Since all three are first order QCD results they depend on the scale of α_s. In order to illustrate the magnitude of the three partial widths for $\gamma + n\,jets$, $n = 1, 2, 3$ and their dependence on the resolution parameter y, we show in Fig. 4 the quantities $10^3\,\Gamma(Z \to \gamma + n\,jets)/\Gamma(Z \to hadrons)$ for $n = 1, 2, 3$ as a function of y and for $\alpha_s(M_Z^2) = 0.118$ [8]. Curves for the KL and KL' scheme are plotted in the cases $n = 1, 2$. The $(\gamma + 3\,jet)$-rate does not depend on the variable scheme since it is a tree graph result. We see that $\Gamma(Z \to \gamma + 2\,jets)$ is dominant and decreases with increasing y as the 3-jet rate does. The width for $Z \to \gamma + 3\,jets$ is strongly y dependent and is appreciable only for small y cut values. $\Gamma(Z \to \gamma + 1\,jet)$ is small and vanihes for $y \to 0$. The predictions for $\Gamma(Z \to \gamma + 2\,jets)$ and $\Gamma(Z \to \gamma + 1\,jet)$ do not depend too strongly on the scheme. The rates in the KL scheme are somewhat larger than in the KL' scheme.

Since our results are only obtained up to $O(\alpha_s)$ one should choose a smaller scale than M_Z^2 in α_s to compensate for unknown higher order effects. This leads to a larger α_s than chosen above and has the effect that the partial width for $\gamma + 3\,jets$ will be larger, the width for $\gamma + 2\,jets$ will slightly decrease and $\Gamma(Z \to \gamma + 1\,jet)$ will decrease for small y and increase slightly for large y. This was found to be true for the KL' scheme which we prefer since in this scheme we expect hadonization corrections to be smaller than in the KL scheme as was found in multi-jet analysis [9,8]. Since the dependence on the scale of α_s is not very strong, we conclude that even higher order corrections in $\Gamma(\gamma + 1\,jet)$ and $\Gamma(\gamma + 2\,jets)$ are moderate. A lowest order α_s has been deduced from the 3-jet rate by comparing data with the $O(\alpha_s)$ formula [6]. Indeed a larger value of α_s has been found corresponding to a decrease of the scale in α_s. See also the contribution of C. Markus [2].

The rates for $Z \to \gamma + 3\,jets$ and $Z \to \gamma + 2\,jets$ shown in Fig. 4 agree with the experimental data [6]. However the result for $Z \to \gamma + 1\,jet$ is smaller than the experimental data of the

OPAL-Collaboration. Experimentally the rate for $\gamma + 1\,jet$ at large y is approximately a factor of 3 to 4 larger than the prediction in Fig. 4. Only for small $y \leq 0.05$ the theoretical curve is consistent with the data. This discrepancy has its origin in the different event definition of the experimental analysis. Experimentally the events were selected in two steps. First only the hadrons were grouped into jets according to a chosen y_{cut} value and then the minimum jet-photon mass was determined. For the $(\gamma + 1\,jet)$-sample the second step had no effect since the hadrons were grouped into one jet with fixed momentum balancing the recoiling photon. Therefore in this sample only the original photon-hadron isolation cut was effective. The exact simulation of the photon isolation cut is not possible since we have not taken the hadronization of the QCD jets into account. To account for the small photon isolation cut in the experimental selection procedure we have calculated the rate for $Z \to \gamma + 1\,jet$ with $y_0 = 0.005$ as the invariant mass cut between photon and the original two jets (e. g. q and $\bar{q}$ in lowest order) which are combined into one jet with the varying mass resolution cut y. For this choice we obtained the dashed-dotted curve in Fig. 4 which now at large y is more than a factor of three larger than the original curve where $y_0 = y$ (no extra photon-jet isolation cut). This agrees well with the data of the OPAL-Collaboration [6]. See also the contribution of C. Markus for further discussions on this "discrepancy" [2]. The effect of the low photon-jet isolation cut can be seen quite clearly already in lowest order and is not a specific feature of the $O(\alpha_s)$ correction term $g_1^{(1)}(y)$.

4 Relation of Decays into Multijets to Rates into One Photon Plus Jets

From the presentation of the previous section it is clear that relations between the rates for $Z \to 4\,jets$ and $Z \to \gamma + 3\,jets$ as well as between $Z \to 3\,jets$ and $Z \to \gamma + 2\,jets$ exist. As was explained above, the decay rate $\Gamma(Z \to \gamma + 3\,jets)$ in lowest order $(O(\alpha\alpha_s))$ equals the C_F^2-part of $\Gamma(Z \to 4\,jets)$ in $O(\alpha_s^2)$ up to known factors involving α and α_s. The 4-jet rate is dominated in this order by the C_F^2 term, the other colour factors $C_F N_c$ and $C_F T_R$ contribute only a fraction to the 4-jet rate [4]. In the future when the data sample for $Z \to \gamma + 3\,jets$ is increased the dominance of the C_F^2 term in $\Gamma(Z \to 4\,jets)$ could be checked by comparing with $\Gamma(Z \to \gamma + 3\,jets)$. Also with more statistics in the $\gamma + 3\,jets$ sample the differential distributions can be used to disentangle the contributions of the three colour factors in $Z \to 4\,jets$ [3]. This is also of interest in order to see effects of higher order $(O(\alpha\alpha_s^2))$ corrections in $\gamma + 3\,jets$ and of $O(\alpha_s^3)$ corrections in 4 jets which have new colour factors as compared to the $O(\alpha\alpha_s)$ and $O(\alpha_s^2)$ contributions, respectively.

The comparison of $\Gamma(Z \to 3\,jets)$ with $\Gamma(Z \to \gamma + 2\,jets)$ is more promising. First the rate for $Z \to \gamma + 2\,jets$ in lowest order is identical to the 3-jet rate up to known factors, i.e. the $g_2^{(0)}(y)$ gives, up to factors involving α_s etc., the hadronic 3-jet rate in $O(\alpha_s)$. In $O(\alpha_s^2)$ the 3-jet rate contains all three colur factors with comparable contributions whereas the $(\gamma + 2\,jet)$-rate in $O(\alpha\alpha_s)$ has only the C_F^2 term. The C_F^2 terms in $\Gamma(Z \to 3\,jets)$ and $\Gamma(Z \to \gamma + 2\,jets)$ are almost equal (they differ only by the extra terms where the two gluons are recombined inside the resolution cut) and therefore cancel in the ratio up to $O(\alpha_s^2)$. To see this we write the hadronic 3-jet width

$$\frac{\Gamma(Z \to 3\,jets)}{\Gamma(Z \to hadrons)} = \frac{1}{1 + \frac{\alpha_s}{\pi} + 1.42(\frac{\alpha_s}{\pi})^2} \frac{\alpha_s}{2\pi} C_F \left(B + \frac{\alpha_s}{2\pi}[C_F\, h_C + N_c\, h_N + T_R\, h_T]\right) \quad (12)$$

where B is the lowest order term $B = g_2^{(0)}(y)$. For the ratio

$$r = \frac{\Gamma(Z \to 3\ jets)}{\Gamma(Z \to \gamma + 2\ jets)} \frac{\frac{\alpha}{2\pi}(\frac{8}{9}c_u + \frac{1}{3}c_d)}{\frac{\alpha_s}{2\pi}C_F(2c_u + 3c_d)} \tag{13}$$

we obtain

$$r = 1 + \frac{\alpha_s}{2\pi}\frac{N_c h_N + T_R h_T}{B + \frac{\alpha_s}{2\pi}C_F h_C}. \tag{14}$$

In (14) we assumed that the h_C contribution is the same for $Z \to 3\,jets$ and $Z \to \gamma + 2\ jets$. The ratio r as given by (14) is plotted in Fig. 5 as a function of y with $\alpha_s = 0.118$ as dashed curve. We see that r increases with decreasing y. Its value above 1 is a measure of the second term in (14) which is dominated by the N_c term and which is positive. This term is a measure of the non-abelean character of QCD. If we choose $N_c h_C = 0$ in (14), this way simulating an "abelean QCD", we obtained the dashed-dotted curve in Fig. 5. Then r is below 1 and decreases with decreasing y as expected since the $T_R h_T$ term is negative. Therefore measurement of r as a function of y is an interesting check related to the non-abelean nature of QCD. The exact result for the ratio r in (13) is the full curve in Fig. 5. The deviation from the dashed curve is small, being significant only for $y \leq 0.05$, where the difference of the h_C term in $g_2(y)$ and in the 3-jet width is not negligible anymore. This comparison is done for the KL' scheme. In the KL scheme we expect similar results. The ratio r has been used in [6] to obtain α_s from the data. The y-dependence of r as shown in Fig. 5 is also nicely reproduced by the data [6].

5 Monte Carlo Implementation

The calculation of $n\,jet$ rates (with or without a photon) to higher orders in QCD involves an integration over high-dimensional phase space regions. An analytical integration or the application of conventional numerical integration methods is succesful only for very specific definitions of $n\,jet$ phase space regions and those prescriptions that can be treated analytically in general do not correspond directly to experimental selection criteria for $\gamma + n\,jets$ events. In order to establish the contact between theoretical predictions and experimental data it is necessary to use more flexible methods as for example the Monte Carlo integration and event generation. In our case this is all the more required as a strong dependence on the experimental selection criteria, i.e. the recombination or cluster algorithm, seems to exist, at least for the $\gamma + 1\,jet$ final state. In the following we will describe the implementation of the matrix element calculation described before into a Monte Carlo event generator.

The application of a Monte Carlo integration is not directly possible since the cross section is singular and strongly peaked at the phase space boundaries $y_{13} = 0$, $y_{14} = 0$, etc.[1] The singular regions have to be isolated and treated analytically in order to obtain a finite result. Moreover, kinematic variables have to be identified which describe the peaking behaviour in a simple way such that variable transformations can be found which render the cross section flat. The essential modelling of the cross section formula has been done already in [4]. There, after a partial fractioning, eq. (11) was obtained where for each contribution one single variable describes the singular behaviour of the cross section. E.g. in the first part of eq. (11) the simple cut $y_{14} \geq y_0$ isolates the singularity. For $y_{14} \leq y_0$ the integration can be performed analytically. After

[1] We need not discuss the terms $\propto y_{23}^{-1}$ and y_{24}^{-1} separately since quark and anti-quark are treated as not distinguishable.

combination with virtual corrections this leads to the $O(\alpha_s)$ corrected cross section for three-parton final states. The Monte Carlo simulation of $q\bar{q}\gamma g$ final states has then to be performed in the remaining region $y_{14} \geq y_0$. Here the transformation $y_{14} \to \ln y_{14}$ removes the dangerous peaking behaviour and the application of Monte Carlo techniques is straightforward. Consequently, our Monte Carlo generates two kinds of events:

(i) In the first channel, $q\bar{q}\gamma$ final states are generated according to the corrected cross section, i.e. including $O(\alpha_s)$ virtual corrections and the singular and non-singular contributions from integrating the $q\bar{q}\gamma g$ cross section over the regions $y_{14} \leq y_0$. Since we choose y_0 very small, $y_0 \simeq O(10^{-4})$, the non-singular parts with $y_{14} \leq y_0$ can actually be neglected.

(ii) Another channel generates $q\bar{q}\gamma g$ events according to the cross section eq. (10) in the phase space region $y_{13} \geq y_0$, $y_{14} \geq y_0$. This corresponds to part (iii) of the preceeding sections. Actually, there are two channels for $q\bar{q}\gamma g$ events: one generates events according to the term proportional to y_{13}^{-1} and the other according to the term $\propto y_{14}^{-1}$.

The $q\bar{q}\gamma g$ events can then be fed into a cluster algorithm which separates events containing an isolated photon from events without an isolated photon and which classifies the photonic events according to the number of jets. The cluster algorithm can use any physical cutoff which need not necessarily be defined in terms of invariant masses $y_{ij}s$, but may involve cuts on energies and angles and may as well treat the separation of photons from jets differently from the separation of two jets. We stress that y_0 is an unphysical cutoff. In order to have a large freedom in the choice of physical cuts and for the separation of $\gamma + n\,jets$ phase space regions, one should take y_0 small enough such that the region $y_{13} \leq y_0$ ($y_{14} \leq y_0$, resp.) cannot contribute to the $\gamma + 3\,jets$ sample.

The basic idea of constructing this kind of Monte Carlo is very simple and well-known in the context of Monte Carlos for QED radiative corrections. There also, events are generated in non-radiative and radiative channels separated with the help of an unphysical small cutoff on the photon energy, usually denoted as k_0, and only afterwards a decision is taken whether the photon can actually be detected in a specific experiment.

However, in practice two problems may occur. The first is related to the fact that the sum of virtual and singular real corrections to the $q\bar{q}\gamma$ cross section are usually negative and can become very large. In some phase space regions and for very small y_0 the magnitude of these negative corrections may even exceed the lowest order cross section, leading to negative values of the $O(\alpha_s)$ corrected cross section. The occurence of events with negative weights has of course to be excluded, either by restricting the phase space in an appropriate way or by using a not so small y_0. Nevertheless, one may still use the Monte Carlo in this case as a tool to numerically calculate the integrated cross section.

The second problem is very specific to our case of photonic $n\,jets$ rates and due to the fact that photons and gluons do behave differently. Consider the singular part coming from the integration of the y_{13}^{-1} pole term in the region $y_{13} \leq y_0$. In this region the quark is not separated from the photon. Moreover, theory prescribes that this singular contribution has to be combined with virtual QED corrections to the $q\bar{q}$ cross section in order to arrive at a finite result. The sum of these two contributions does therefore not contribute to the $(\gamma + n\,partons)$-cross section. However, experimentally one does not observe partons but hadron jets and the separation of photonic events from non-photonic ones has to be defined in terms of the full hadronic final state kinematics. It may well happen that events with $y_{13} \leq y_0$ after hadronization of the quark are classified as

photonic events. This is so since configurations with $y_{13} = 0$ correspond to i) events with a soft photon, or ii) events with a collinear quark-photon pair, or iii) events with a soft quark and a hard photon. The latter case will lead with a certain probability depending on the hadronization model to events with a hard isolated photon, the soft quark being dragged to a near-by jet of the anti-quark or a gluon. It is clear from this consideration that the separation of photonic events from non-photonic ones may be very sensitive to the fragmentation and hadronization model. The important consequence for the Monte Carlo implemenatation of the matrix element calculation is that although the total generated cross section is independent on y_0, the separation into $\gamma + 1$-, 2-, and 3 *jets* events may not. The independence on y_0 for $\gamma + n$ *jets* rates is guaranteed only when the phase space boundaries separating the corresponding regions one from another do never reach the singular regions $y_{13} \leq y_0$, $y_{14} \leq y_0$.

That this is not automatically the case may be explained for the simpler case of $q\bar{q}\gamma$ final states, i.e. without QCD corrections, and the $\gamma + 1$ *jet* cross section. Here singularities appear for $y_{23} = 0$ or $y_{13} = 0$ and they have to be excluded by cuts $y_{23} \geq y_0$ and $y_{13} \geq y_0$. Now consider the following cluster algorithm:

i) calculate the invariant masses y_{ij} for any pair of particles (hadrons or photons);

ii) take the pair with smallest y_{ij} and recombine it into a cluster if $y_{ij} \leq y$. y is a physical cut, $y \gg y_0$;

iii) repeat steps i) and ii) until all y_{ij} are larger than y;

iv) select $\gamma + n$ *jets* events by taking only those events which contain a cluster that consists of a single photon, i.e. where the photon has not been combined with another particle or cluster during steps i) – iii).

The phase space region defined by this algorithm for the $\gamma + 1$ *jet* cross section applied to the $q\bar{q}\gamma$ case is shown in Fig. 6. It is defined by $y_{12} \leq y_{13}$, $y_{12} \leq y_{23}$, and $y_{12} \leq y$ and extends into the corners $x_1 = 1$, $x_2 = 1$ which are however excluded by the requirement $y_{13} \geq y_0$, $y_{23} \geq y_0$. Inside these bands also shown in the figure, the calculation is done analytically to obtain the singular part which is combined with virtual corrections and contributes to QED radiative corrections to $q\bar{q}$ production. Only the triangular region $y_{13} \geq y_0$, $y_{23} \geq y_0$ (i.e. $x_1 \leq 1 - y_0$, $x_2 \leq 1 - y_0$, $x_1 + x_2 \geq 1$) is considered as genuine $q\bar{q}\gamma$ events that are treated in the cluster algorithm. Obviously there is a mismatch in these corners. In this simple case the problem is not too severe since the contribution to the cross section coming from these corners is finite and of order $O(y_0)$ only. However, for the $q\bar{q}\gamma g$ case, since the phase space is higher-dimensional, the cross section coming from the analogous corners is divergent of the order of $O(\ln y_0)$.

A cluster algorithm like this is therefore not allowed. A simple solution is to directly require the photon isolation with respect to any particle, not just from jets which are already clusters of particles. For example:

i) select $\gamma + n$ *jets* events by requiring the invariant mass of the photon with any particle in the event to be larger than a cutoff, $y_{i\gamma} \geq y_\gamma$;

ii) apply a cluster algorithm to the hadronic part of the event;

iii) separate $\gamma + 1$-, 2-, and 3 *jets* events by the number of remaining clusters of hadrons.

In order to study the influence of specific cluster and recombination algorithms, one has thus to use a full Monte Carlo which also simulates the hadronization of the final state quarks and gluons. For this article we restrict ourselves to a discussion of numerical results obtained from the Monte Carlo simulation of the final state on the parton level, i.e. of $q\bar{q}\gamma$ and $q\bar{q}\gamma g$ events[2]. The program was checked by recalculating the results of Kramer and Lampe reviewed in the first part of this article. For this, $\gamma+1$-, 2-, and 3 *jets* events have been identified according to phase space regions defined in terms of y_{ij} and y_{ijk} as explained in [4]. We found complete agreement between the two aproaches. For the study of other recombination schemes on the level of partonic events without running into the problem of obtaining y_0 dependent $\gamma + n$ *jets* rates, it is necessary to exclude the contribution from the y_{13}^{-1}-pole term. The quality of this approximation was checked within the KL and KL' recombination schemes. There we found that at small y ($\simeq 0.01$) the y_{13}^{-1}-pole part contributes about 15 % to $g_2(y)$ but at larger values $y \geq 0.1$ the approximation is good to about 5 %. Thus the y_{13}^{-1}-pole term is not dominant in the $\gamma + 2$ *jets* rate, however we expect the approximation to be worse for the $\gamma + 1$ *jet* rate.

In Fig. 7 we show the (γ+2 *jets*)-rate $\Gamma(Z \to \gamma + 2\,jets)$ normalized to $10^{-3}\Gamma(Z \to hadrons)$ as obtained from the Monte Carlo for the KL and KL' scheme compared with results for the recombination schemes usually denoted by E and E0. In the E scheme, two partons are combined to a jet by adding the 4-momenta if $y_{ij} \leq y$ and in the E0 scheme the energies of the two particles are added but the sum of the spatial momenta is rescaled in order to obtain a massless jet. It is seen from the figure that the E scheme gives results in agreement with the KL prescription whereas the E0 recombination gives results very close to the KL' scheme. Other recombination schemes (P and P0, e.g.) are very similar to the E0 scheme. This is in accordance with results for the 3-jet rate [9].

The Monte Carlo can be used to study the influence of the jet resolution cut and the photon isolation cut separately. Fig. 8 presents results for the ($\gamma + 2$ *jets*)-rate in the E scheme as a function of a cut y_γ which was used to identify events with an isolated photon by requiring $y_{i3} \geq y_\gamma$ for $i = 1,\ 2,\ 4$ while keeping a fixed value for the jet resolution cut, denoted by y_J. It is seen that the result depends strongly on y_γ and for large $y_J \geq 0.05$ the photon isolation cut is dominating the cut dependence. This demonstrates that a careful matching of experimental and theoretical prescriptions for the selection of photonic events is necessary.

[2]The Monte Carlo event generator GNJETS is now available including an interface to routines from JETSET 7.3 for fragmentation and hadronization of the final state.

Figure Captions

Fig. 1: Lowest order Feynman diagrams for Z decay into $q\bar{q}\gamma$.

Fig. 2: Example of a Feynman diagram for $Z \to q\bar{q}\gamma g$ with labelling of momenta.

Fig. 3: Scheme dependence of higher order coefficients $(O(\alpha_s^2))$ $g_{32}(y)$ in $Z \to 3\ jets$ and $(O(\alpha\alpha_s))$ $g_2^{(1)}(y)$ in $Z \to \gamma + 2\ jets$ for the KL and KL' scheme.

Fig. 4: Partial widths $\Gamma(Z \to \gamma + n\ jets)$ (n=1,2,3) as a function of y for $\alpha_s = 0.118$ and normalized with $10^{-3}\Gamma(Z \to hadrons)$ for the KL and KL' scheme. $\Gamma(Z \to \gamma + 1\ jet)$ is also given for a small photon-jet isolation cut $y_0 = 0.005$ (dashed-dotted) curve.

Fig. 5: The ratio r, the reduced hadronic 3-jet width divided by the reduced $(\gamma+2\ jet)$-width as a function of y in the approximation (14) (dashed curve), for "abelean QCD" (dashed-dotted curve) and calculated from the theoretical 3-jet width and the $(\gamma + 2\ jet)$-width (full curve).

Fig. 6: Phase space for $q\bar{q}\gamma$ final states with the $\gamma + 1\ jet$ region from a cluster algorithm as described in the text.

Fig. 7: Monte Carlo results for the partial width $\Gamma(Z \to \gamma+2\ jets)$ as a function of y normalized to $10^{-3}\Gamma(Z \to hadrons)$, $\alpha_S = 0.118$, for various recombination schemes. The y_{13}^{-1} pole contribution is neglected in this figure.

Fig. 8: Monte Carlo results for the partial width $10^3\Gamma(Z \to \gamma + 2\ jets)/\Gamma(Z \to hadrons)$ as in fig. 7 for the E scheme recombination as a function of the photon y cut y_γ for fixed values of the jet resolution y cut $y_J = 0.01$, 0.05, and 0.1. The y_{13}^{-1} pole contribution is neglected in this figure.

References

[1] P. Mättig, W. Zeuner, Z. Phys C52 (1991) 37

[2] C. Markus: Experimental Results on Matrix Element Calculations; these proceedings

[3] P. Mättig: Studies of $q\bar{q}g\gamma$ versus Four Jets; these proceedings

[4] G. Kramer, B. Lampe, Fortschr. Phys. 37 (1989) 161

[5] G. Kramer, B. Lampe, DESY 91-78 and a shorter version in Phys. Lett. B269 (1991) 401

[6] OPAL collaboration, M. Z. Akrawy et al., Phys. Lett. B253 (1991) 511; OPAL Collaboration, P. Acton et al., CERN-PPE/91-189

[7] F. Gutbrod, G. Kramer, G. Rudolph, G. Schierholz, Z. Phys. C35 (1987) 543

[8] OPAL Collaboration, M. Z. Akrawy et al., Z. Phys. C49 (1991) 375

[9] G. Kramer, N. Magnussen, Z. Phys. C49 (1991) 301

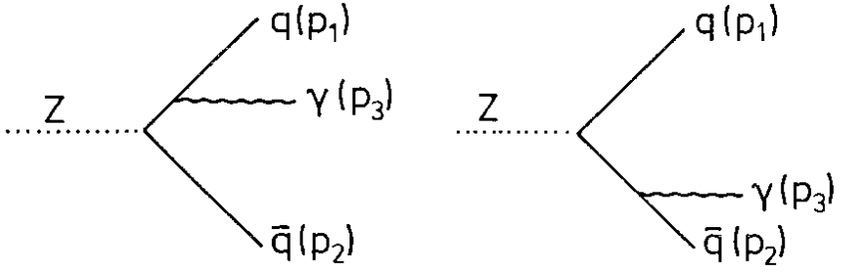

Fig. 1

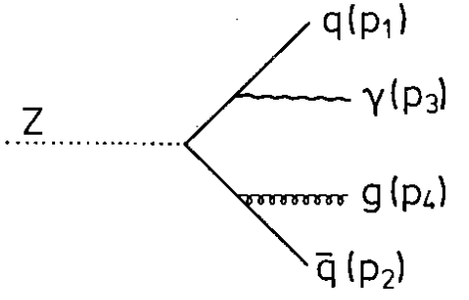

Fig. 2

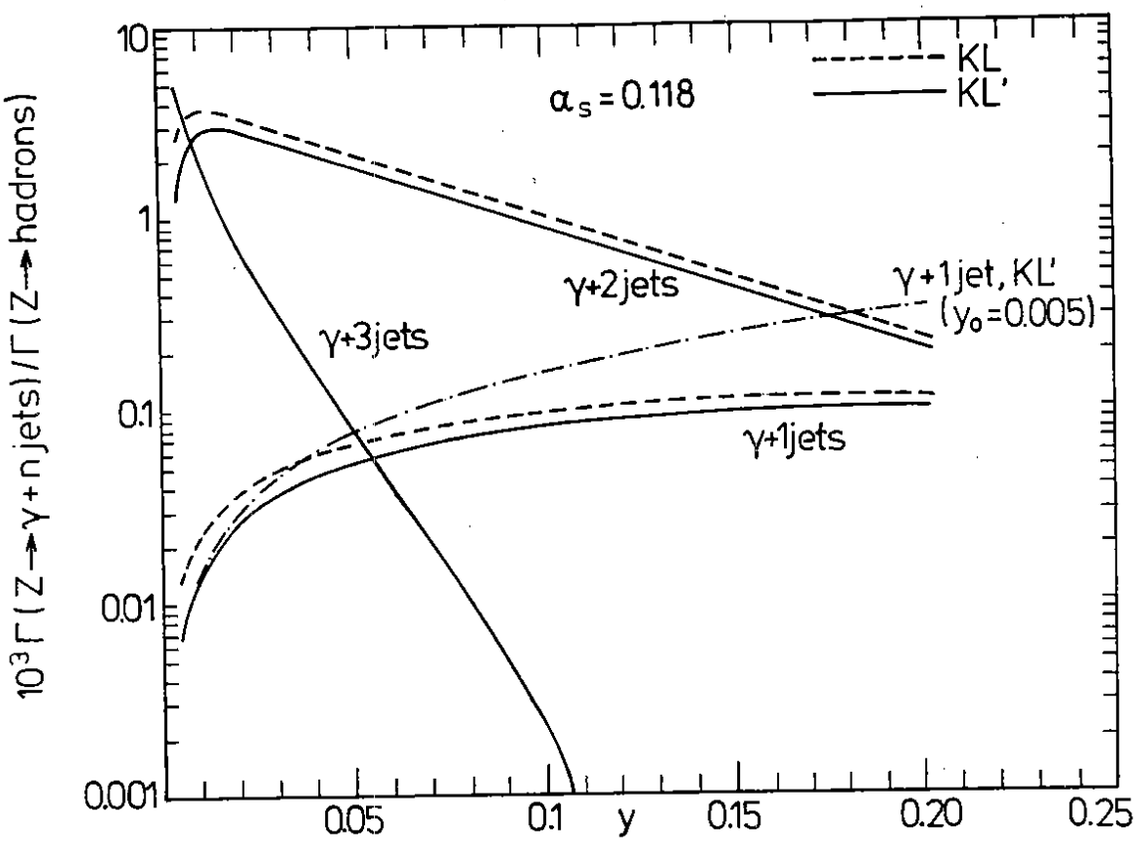
$10^3\Gamma(Z\to\gamma+n\,\text{jets})/\Gamma(Z\to\text{hadrons})$
10
1
0.1
0.01
0.001
$\alpha_s = 0.118$
KL
KL'
γ+2jets
γ+1jet, KL'
(y_0=0.005)
γ+3jets
γ+1jets
0.05
0.1
y
0.15
0.20
0.25

Fig. 4

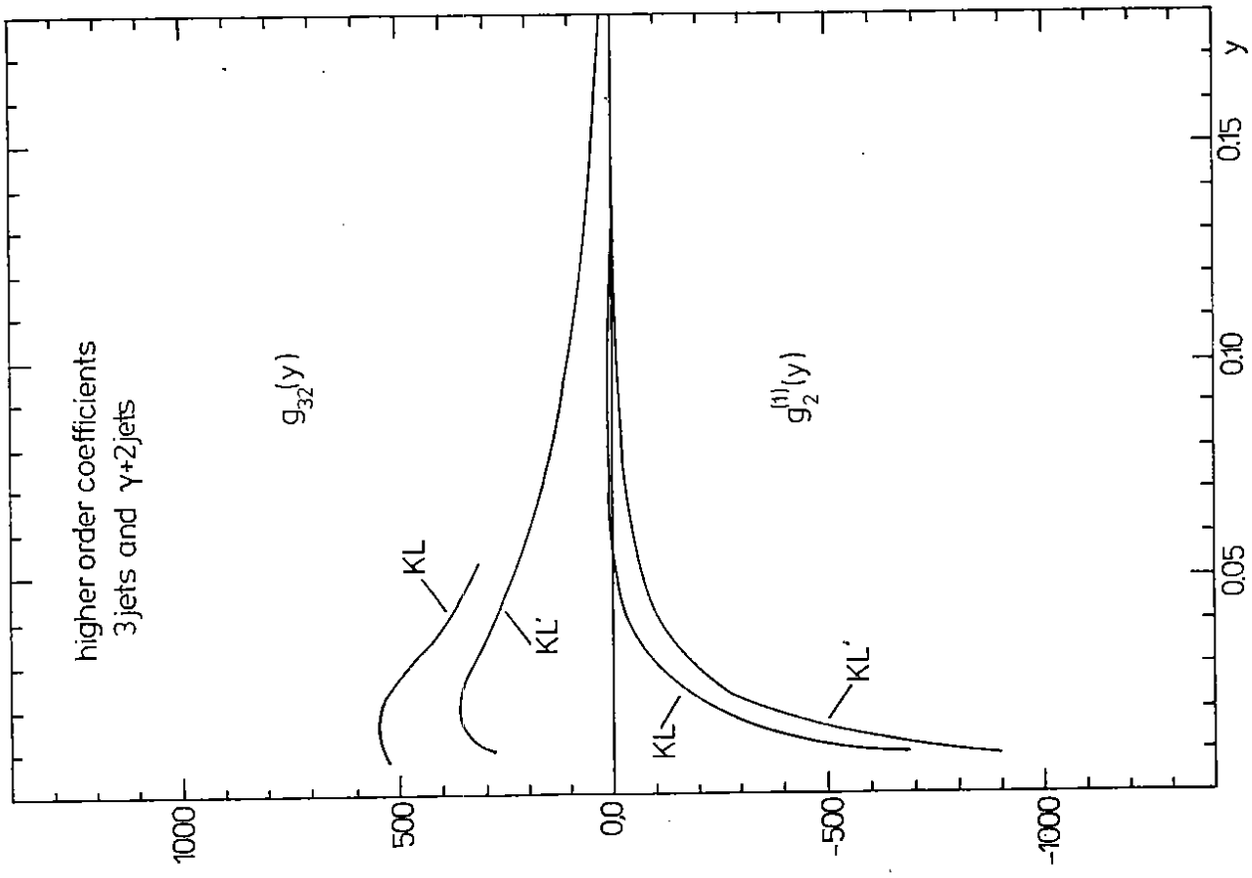
higher order coefficients
3 jets and γ+2jets
$g_{32}(y)$
$g_2^{(1)}(y)$
KL
KL'
KL
KL'
1000
500
0.0
-500
-1000
y
0.15
0.10
0.05

Fig. 3

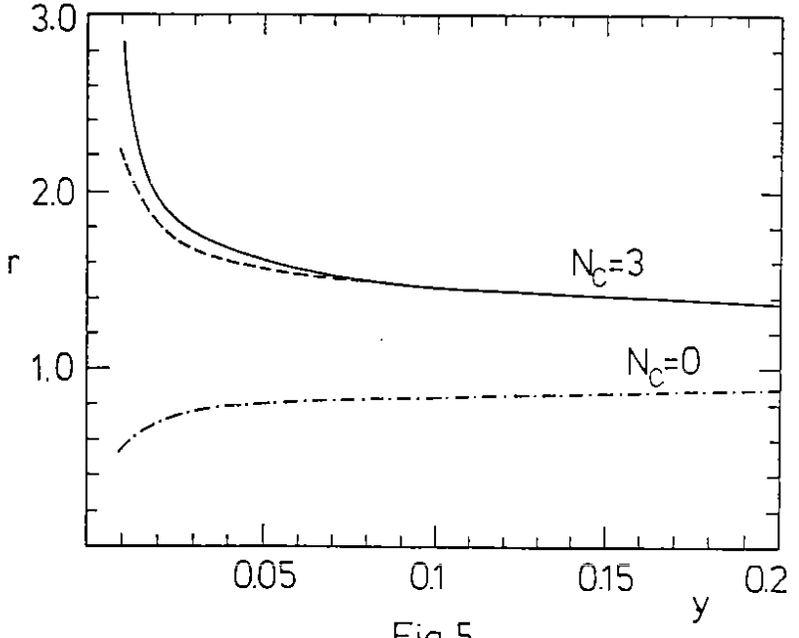

Fig. 5

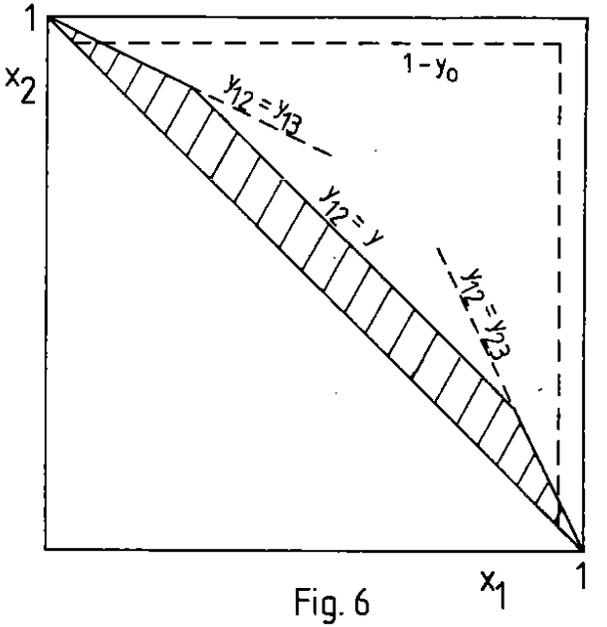

Fig. 6

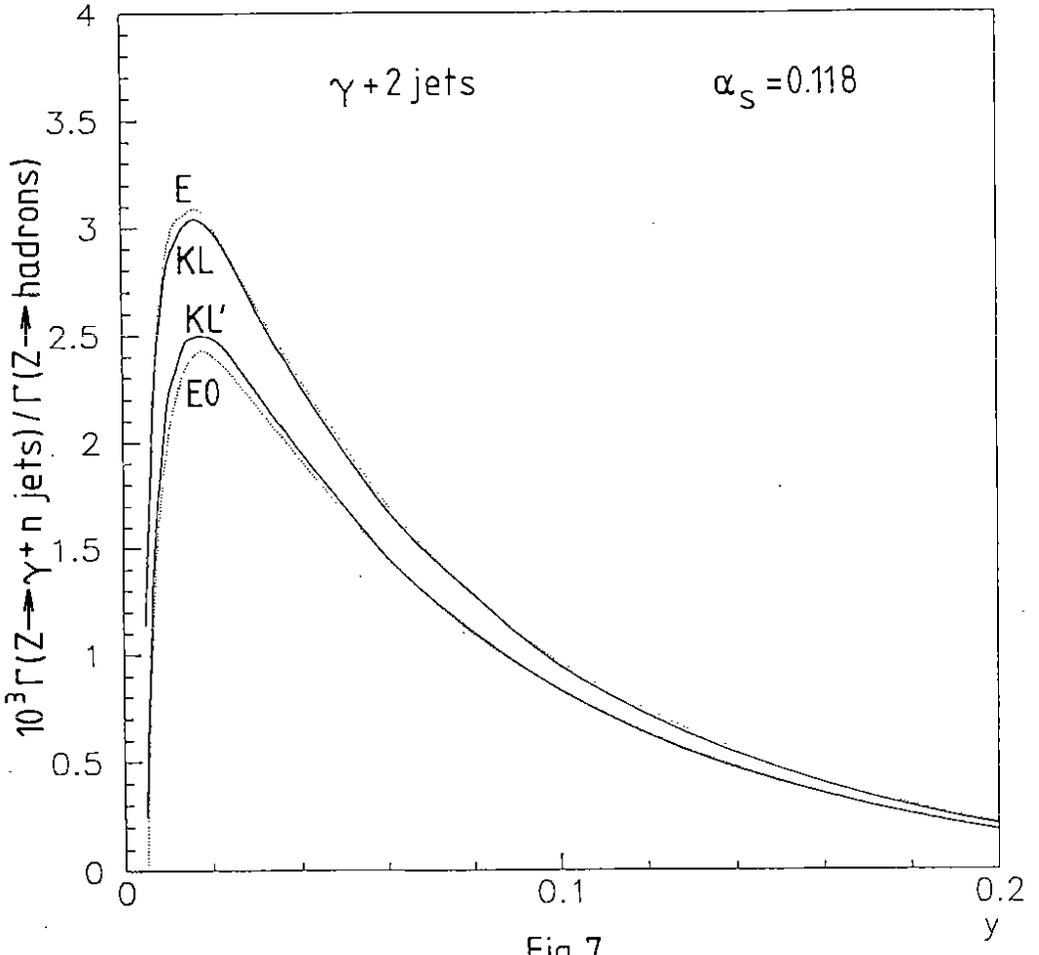
γ + 2 jets
α_s = 0.118
E
KL
KL'
E0
$10^3 \Gamma(Z \to \gamma + n\ \text{jets}) / \Gamma(Z \to \text{hadrons})$
y
0
0.1
0.2
0.5
1
1.5
2
2.5
3
3.5
4

Fig.7

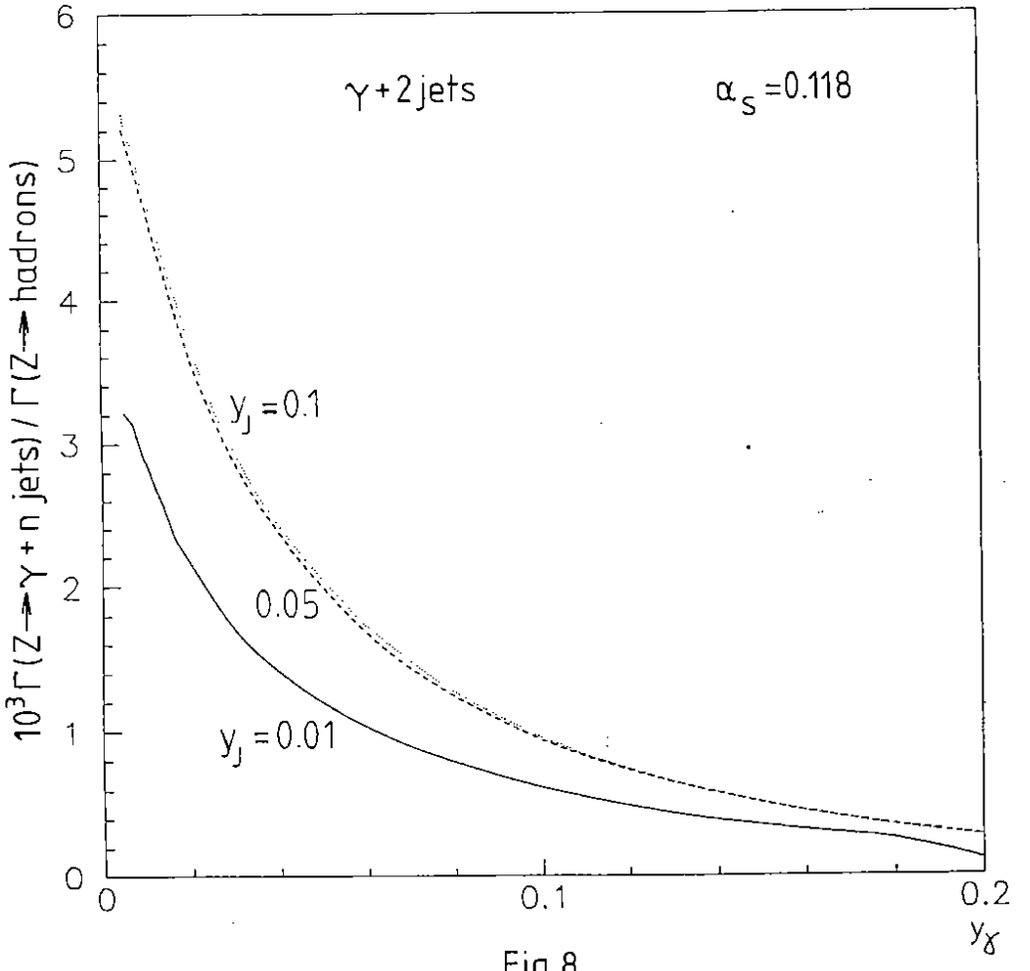
γ + 2 jets
α_s = 0.118
y_j = 0.1
0.05
y_j = 0.01
$10^3 \Gamma(Z \to \gamma + n\ \text{jets}) / \Gamma(Z \to \text{hadrons})$
y_γ
0
0.1
0.2
1
2
3
4
5
6

Fig.8